Advanced Powder Technology xxx (2016) xxx–xxx

Contents lists available at ScienceDirect

Advanced Powder Technology

journal homepage: www.elsevier.com/locate/apt

Original Research Paper

Numerical simulation of water based magnetite nanoparticles between two parallel disks

Rizwan Ul Haq [a,*], N.F.M. Noor [b], Z.H. Khan [c]

[a] Department of Mathematics, Quaid-i-Azam University, Islamabad 44000, Pakistan
[b] Institute of Mathematical Sciences, Faculty of Science, University of Malaya, 50603 Kuala Lumpur, Malaysia
[c] Department of Mathematics, University of Malakand, Dir (Lower), Khyber Pakhtunkhwa, Pakistan

A R T I C L E I N F O

Article history:
Received 12 October 2015
Received in revised form 11 April 2016
Accepted 20 May 2016
Available online xxxx

Keywords:
Squeezing channel
Magnetite nanoparticles
Thermal conductivity
Numerical solution

A B S T R A C T

Present study examines the fully developed squeezing flow of water functionalized magnetite nanoparticles between two parallel disks. For strongly magnetite fluid three different types of nanoparticles having better thermal conductivity: Magnetite (Fe_3O_4), Cobalt ferrite ($CoFe_2O_4$) and Mn–Zn ferrite (Mn–$ZnFe_2O_4$) are incorporated within the base fluid (water). Systems of equations containing the nanoparticle volume fraction are rehabilitating in the form of partial differential equations using cylindrical coordinate system. Resulting mathematical model is rehabilitated in the form of ordinary differential equations with the help of compatible similarity transformation. Results are analyzed for velocity, temperature, reduced skin friction and reduced Nusselt number with variation of different emerging parameters and determine the superb thermal conductivity among mentioned nanoparticles. Comparison among each mixture of ferrofluid has been plotted as response to differences in reduced skin friction and reduced Nusselt number distributions. Dominating effects are analyzed for squeezing parameter and it is found that water based-magnetite (Fe_3O_4) gives the highest reduced skin friction and reduced Nusselt number as compared to the rest of the mixtures. Isotherms are also plotted against various values of nanoparticle volume fraction to analyze the temperature distribution within the whole domain of squeezing channel.

1. Introduction

Squeezing flow is a term frequently addressed in practical environments to define a fluid movement along a contracting domain of a prescribed length. Such flow can be set up by positioning an initial stagnant fluid between two parallel rectangular plates and disks or even in a channel to represent the corresponding mathematical models on specific coordinate planes. Hence the squeezing flow is generalized when the fluid is suppressed to pass through the commonly horizontally narrow enclosure due to one of the surface contracting vertically in relation to the other stationary surface. Adversely there are generous studies incriminating a contracting rotating disk as well as two rotating disks or two moving walls toward or away from each other. Research interests in squeezing flows are rapidly developed due to existing and growing applications in the transport of biological fluids and in the manufacturing processes of polymer, lubrication, hydrodynamic compression, purification, filtration, injection molding and many others. Squeezing motion at varying distance between two moving disks is inspected by Ishizawa [1] using a perturbative solution. Moreover, Usha and Sridharan [2] derive an exact solution for similar pertinent factor but between two elliptic plates in the form of infinite time-dependent multifold series. The squeezing flow of couple stress fluid through an elongated rectangular channel is solved numerically by Srinivasacharya et al. [3] via a generalized Newton's method. They observed increment in radial velocity near the central plane when the wall expansion ratio increases. Recently, many authors contribute in the development of squeezing flow for different fluid models [4–7].

Recently Khan et al. [8] did a method convergence study for a unidirectional axisymmetric squeezing flow by employing variation of parameters method (VPM) as compared to the fourth-order Runge–Kutta (RK) method and homotopy analysis method (HAM). They asserted that VPM converges at fifth-order solution while HAM converges at seventh order for the two-dimensional problem between two parallel plates. Later they extended the analysis to investigate the influence of magnetohydrodynamics (MHD) using VPM [9]. Numerical solution based on a three-stage finite difference formula for a viscous fluid between contracting rotating disks is provided by Nazir and Mahmood [10]. Taking into account the viscous dissipation effects in the energy equation and rotating

* Corresponding author. Tel.: +92 333 5371853.
E-mail addresses: ideal_riz@hotmail.com, r.haq.qau@gmail.com (R. Ul Haq).

http://dx.doi.org/10.1016/j.apt.2016.05.020
0921-8831/© 2016 Published by Elsevier B.V. on behalf of The Society of Powder Technology Japan.

porous heated disks, Si et al. [11] solved the fluid flow with the help of HAM. It is drawn that sufficiently large rotation can dominate the squeezing flow radial velocity field over the permeability Reynolds number. Moreover Si et al. [12] discovered that the stream-wise velocity and the temperature of a micropolar fluid flow in a porous channel are of increasing functions of micropolar parameter in the presence of suction at two expanding/contracting walls. The effects of Dufour (diffusion-thermo) and Soret (thermal diffusion) commenced as the energy flux is inducted by composition gradient and mass flux is devised by temperature gradient respectively between two contracting rotating porous disks have been considered by Srinivas et al. [13] while Fang et al. [14] examined the unsteady flow outside a contracting cylinder where a unique non-trivial solution has been found.

Choi [15] is the first researcher who introduced the brief terminology of nanofluids to refer regular fluids suspended with solid nano-sized particles possibly via two specific preparation methods. The thermal and transport properties of these base fluids are highly influenced by the stable suspended nanoparticles. Timeless demands in acquiring, producing and utilizing regular fluids for prominent enhancement in heat transfer and conductivity have boosted up research and technical publications related to nanofluids and still. Complete transport model for nanofluid flow under slip condition is primarily proposed by Buongiorno [16] based on seven assumptions while treating nanofluid as a two-component mixture. Natural convection of micropolar nanofluids in a square cavity is modeled by Bourantas and Loukopoulos [17]. At the outset, they emphasized the agreement of the proposed theoretical model of single-phase nanofluid flow with numerical solutions obtained from finite volume method and secondly with available experimental data. Extensive review on the heat transfer characteristics of nanofluids is written by Wang and Mujumdar [18]. Rashidi et al. [19] studied buoyancy and thermal radiation correspond to magnetohydrodynamic (MHD) flow over a stretching surface using water as the base fluid suspended with Cu metal and Cu-oxide nanoparticles. Both the skin friction coefficient and the Nusselt number are greater for Cu metal nanofluid compared to Cu-oxide nanofluid. Next, mixed convective flow of Al_2O_3–water nanofluid inside a vertical microtube is analyzed by Malvandi and Ganji [20]. They concluded that Hartmann number, slip and mixed convection parameters enhance heat transfer rate in the nanofluid flow where the impacts are more pronounced as the size of the nanoparticles is reduced. Some current research of nanofluids can be reviewed from [21–31].

Squeezing nanofluid flow is an emerging spectrum of studies from abundant industrial applications of squeezing problems especially when the outcome of products highly affected by the heat transfer rate is of desirable priority. Domairry and Hatami [32] demonstrated that a reduced local Nusselt number can be improved when Eckert number, squeeze parameter and nanoparticle volume fraction are increased in the case of squeezing Cu–water nanofluid flow between parallel disks using DTM-Pade method. The unsteady squeezing nanofluid flow is solved analytically by Sheikholeslami et al. [33] using the Adomian decomposition method (ADM) while Dib et al. [34] compared the approximate analytical solution via Duan–Rach Approach (DRA) with Runge Kutta method for the same model. Least square method is employed by Hatami et al. [35] on an asymmetric flow incorporating Cu, Ag and Al_2O_3 nanoparticles where the flow temperature circulation is spread up with an increment in the squeeze number. The study is further extended as they imposed an externally heated plate while the other plate is injected with a coolant fluid through it [36]. They highlighted that the squeezing flow of copper nanofluid gives the maximum Nusselt number in this model as compared to silver and alumina nanofluids. Recently the squeezing nanofluid flow between two parallel disks in the highlight of variable magnetic field applied perpendicularly on the lower stationary disk with the contracting upper disk is emphasized by Hatami and Ganji [37]. It is observed that higher values of Brownian and thermophoresis parameters contribute to significant hike in both Nusselt and Sherwood numbers. Some recent studies that reflect the better analysis on nanofluid with various geometries are [38–42].

In view of potential applications of squeezing nanofluid flow in scientific and engineering sectors including food, hydraulic and chemical processing equipment as well as for cooling and freezing industries, more updated studies are needed to unclench more characteristics behaviors of such models. Secondly, the available literatures of squeezing nanofluid flows are limited in the extent of breakthrough on more prominent physical parameters, types of fluid and nanoparticles considered, variations of both analytical or numerical methods and also due to the fact that current research of squeezing nanofluid boundary layer flows are mostly dominated by a minority of journals and researchers. Looking at this scenario as motivation and opportunity, the present study is dedicated to consolidate three different types of nanoparticles namely magnetite (Fe_3O_4), cobalt ferrite ($CoFe_2O_4$) and Mn–Zn ferrite (Mn–$ZnFe_2O_4$) saturated within water as the base fluid. The similarity transformation is adopted together with shooting technique and Runge–Kutta–Fehlberg to solve the resulting system of nonlinear ordinary differential equations. Various profiles of velocity, temperature, reduced skin friction and reduced Nusselt number are plotted and discussed including rundown of isotherms of the flow. Finally it is our hope that through the present study, research in this field can be expanded and benefited eminently in the future of broad disciplines.

2. Mathematical model

Consider MHD incompressible water based nanoparticles flowing between two infinitely parallel disks in such a way that the distance between disks remains finite. We have considered three different kinds of Ferro particles: magnetite (Fe_3O_4), cobalt ferrite ($CoFe_2O_4$) and Mn–Zn ferrite (Mn–$ZnFe_2O_4$) within the base fluid (water). It is further assumed that magnetic field $B_o(1-at)^{-1/2}$ is applied normal to the disks and based on the flow assumption due to low Reynolds number, the induced magnetic field is neglected. Constant temperatures T_w and T_h are defined at lower surface $z=0$ and upper surface $z=h(t)$ of the disks respectively. Moreover, it is assumed that upper disk is moving with the velocity $aH(1-at)^{-1/2}/2$ in both directions (toward and away) from the stationary lower plate at $z=0$. Physical description of the model is presented in Fig. 1. The cylindrical coordinate system (r,α,z) is considered and due to the rotational symmetry of the flow $(\partial/\partial\alpha=0)$, the azimuthal component v of the velocity $V=(u,v,w)$ vanishes identically. Thus the governing and energy equations for the unsteady two-dimensional flow of a viscous fluid take the following form [7]

$$\frac{\partial u}{\partial r}+\frac{u}{r}+\frac{\partial w}{\partial z}=0, \tag{1}$$

$$\frac{\partial u}{\partial t}+u\frac{\partial u}{\partial r}+w\frac{\partial u}{\partial z}=-\frac{1}{\rho_{nf}}\frac{\partial p}{\partial r}+\frac{\mu_{nf}}{\rho_{nf}}\left(\frac{\partial^2 u}{\partial r^2}+\frac{1}{r}\frac{\partial u}{\partial r}-\frac{u}{r^2}+\frac{\partial^2 u}{\partial z^2}\right)-\frac{\sigma}{\rho_{nf}}B^2(t)u, \tag{2}$$

$$\frac{\partial w}{\partial t}+u\frac{\partial w}{\partial r}+w\frac{\partial w}{\partial z}=-\frac{1}{\rho_{nf}}\frac{\partial p}{\partial z}+\frac{\mu_{nf}}{\rho_{nf}}\left(\frac{\partial^2 w}{\partial r^2}+\frac{1}{r}\frac{\partial w}{\partial r}+\frac{\partial^2 w}{\partial z^2}\right), \tag{3}$$

$$\frac{\partial T}{\partial t}+u\frac{\partial T}{\partial r}+w\frac{\partial T}{\partial z}=\alpha_{nf}\left(\frac{\partial^2 T}{\partial r^2}+\frac{1}{r}\frac{\partial T}{\partial r}+\frac{\partial^2 T}{\partial z^2}\right). \tag{4}$$

Please cite this article in press as: R. Ul Haq et al., Numerical simulation of water based magnetite nanoparticles between two parallel disks, Advanced Powder Technology (2016), http://dx.doi.org/10.1016/j.apt.2016.05.020

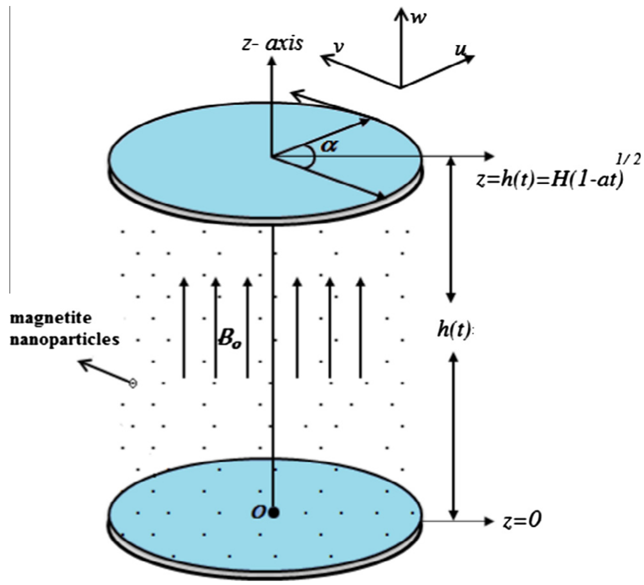

Fig. 1. Geometry of the problem.

In the expressions above, u and w are the velocity components along the r and z-direction respectively, p is the pressure, T is the temperature, ρ_{nf} is the density of nanofluid, μ_{nf} is the dynamic viscosity of nanofluid and k_{nf} is the thermal conductivity of the nanofluid which are defined as

$$\left.\begin{array}{l} \mu_{nf}=\frac{\mu_f}{(1-\phi)^{2.5}},\ \rho_{nf}=(1-\phi)\rho_f+\phi\rho_s,\\ (\rho C_p)_{nf}=(1-\phi)(\rho C_p)_f+\phi(\rho C_p)_s,\ \nu_{nf}=\frac{\mu_{nf}}{\rho_{nf}},\\ \frac{k_{nf}}{k_f}=\frac{(k_s+2k_f)-2\phi(k_f-k_s)}{(k_s+2k_f)+\phi(k_f-k_s)},\ \alpha_{nf}=\frac{k_{nf}}{(\rho C_p)_{nf}}, \end{array}\right\}, \tag{5}$$

with k_s is the thermal conductivity of the solid fraction, k_f is the thermal conductivity of base fluid, ρC_p is the specific heat capacity and ϕ is the solid volume fraction of nanoparticles. The respective boundary conditions are written as

$$\left.\begin{array}{l} u=0,\quad w=\frac{dh}{dt},\quad \text{at}\quad z=h(t)\\ u=0,\quad w=0,\quad \text{as}\quad z\to 0\\ T=T_w\quad \text{at}\quad z=0,\\ T=T_h\quad \text{at}\quad z=h(t). \end{array}\right\}. \tag{6}$$

Here T_w is the temperature of the lower disk at $z=0$ and T_h is the temperature of the upper disk at $z=h(t)$. Introducing the following transformations

$$\left.\begin{array}{l} u=\frac{ar}{2(1-at)}f'(\eta),\quad w=\frac{aH}{(1-at)^{1/2}}f(\eta),\\ B(t)=\frac{B_0}{(1-at)^{1/2}},\ \eta=\frac{z}{H(1-at)^{1/2}},\ \theta=\frac{T-T_h}{T_w-T_h}. \end{array}\right\}, \tag{7}$$

Through Eqs. (2)–(4), eliminating the pressure gradients from the resulting equations we finally obtain

$$\frac{1}{(1-\phi)^{2.5}}f'''' - S\left((1-\phi)+\phi\frac{\rho_s}{\rho_f}\right)(\eta f''' + 3f'' - ff''') - Mf'' = 0, \tag{8}$$

$$\frac{k_{nf}}{k_f}\theta'' + SPr\left((1-\phi)+\phi\frac{(\rho C_p)_s}{(\rho C_p)_f}\right)(2f'\theta - \eta\theta') = 0. \tag{9}$$

with the boundary conditions defined as

$$\begin{array}{lll} f(0)=0, & f'(0)=0, & \theta(0)=1,\\ f(1)=1/2, & f'(1)=0, & \theta(1)=0. \end{array} \tag{10}$$

Here prime denotes derivative with respect to η while S denotes the squeeze number, M the Hartman number and Pr the Prandtl number correspondingly defined as

$$S=\frac{aH^2}{2\nu_f},\quad M=\sqrt{\frac{\sigma B_0^2}{a\rho_f}},\quad Pr=\frac{\mu_f(\rho C_p)_f}{\rho_f k_f}. \tag{11}$$

Physical quantities of interest are the skin friction coefficient and Nusselt number which are defined as:

$$C_f=\frac{\mu_{nf}\left(\frac{\partial u}{\partial z}+\frac{\partial w}{\partial r}\right)_{z=h(t)}}{\rho_{nf}\left(-aH/2\sqrt{1-at}\right)^2},\quad Nu=\frac{k_{nf}\left(\frac{\partial T}{\partial z}\right)_{z=h(t)}}{k_f(T_w-T_h)}. \tag{12}$$

Making use of Eq. (7) in Eq. (12), we get

$$\frac{H^2}{r^2}Re_rC_{fr}=\frac{1}{(1-\phi)^{2.5}\left((1-\phi)+\phi\frac{\rho_s}{\rho_f}\right)}f''(1),\quad (1-at)^{1/2}Nu = -\frac{k_{nf}}{k_f}\theta'(0). \tag{13}$$

Here $Re_r=\frac{\rho_f raH(1-at)^{1/2}}{a\mu_f}$ is the local squeezed Reynolds number.

3. Methodology

The above mentioned coupled differential Eqs. (8) and (9) along with the boundary conditions defined in Eq. (10) are tackled numerically. We have used the fourth-order Runge–Kutta method and this method is a reasonably simple and robust scheme featuring a shooting technique. The Runge–Kutta Method is a method of numerically integrating ordinary differential equations using a trial step at the midpoint of an interval to cancel out lower-order error terms. The step size is taken as $\Delta\eta=0.01$ and the procedure for RKF method is repeated until we get the asymptotically convergent results within a tolerance level of 10^{-6}. All these working schemes are assimilated in the computational software Matlab 14. Mathematical procedure for fourth-order formula is:

$$k_1=hf(x_n,y_n), \tag{14}$$

$$k_2=hf\left(x_n+\frac{1}{2}h,y_n+\frac{1}{2}k_1\right), \tag{15}$$

$$k_3=hf\left(x_n+\frac{1}{2}h,y_n+\frac{1}{2}k_2\right), \tag{16}$$

$$k_4=hf(x_n+h,y_n+k_3), \tag{17}$$

$$y_{n+1}=y_n+\frac{1}{6}k_1+\frac{1}{3}k_2+\frac{1}{3}k_3+\frac{1}{6}k_4+O(h^5). \tag{18}$$

4. Results and discussion

In order to analyze the fluid flow behavior and heat transfer, results have been constructed per axial velocity $f(\eta)$, radial velocity $f'(\eta)$ and temperature profile $\theta(\eta)$ with various values of emerging parameters such as squeezing parameter S, Hartmann number M and nanoparticle volume fraction ϕ. Since the present model has been developed for water based Ferro nanoparticles named as magnetite (Fe_3O_4), cobalt ferrite ($CoFe_2O_4$) and Mn–Zn ferrite ($Mn–ZnFe_2O_4$), subsequent behavior of each mixture remains the same for velocities along the axial and radial coordinates and so in temperature profile. As expressed in Figs. 2–6, outcomes are only plotted for water-based magnetite (Fe_3O_4) particles in relation to velocity and temperature. Before further discussion on the graphical section, it is noted that we are using the thermophysical properties of water and magnetic nanoparticles as mentioned in Table 1. Numerical values of skin friction coefficient and local Nusselt number for each water functionalized $CoFe_2O_4$ particle with the various values of ϕ, M and S are plotted in Tables 2 and 3.

Fig. 2(a) and (b) illustrates the behavior of axial velocity $f(\eta)$ against squeezing parameter S and Hartmann number M respectively. It is observed in Fig. 2(a) that there is insignificant variation in the axial velocity $f(\eta)$ for distinct values of the squeezing parameter S and the nanoparticle volume fraction ϕ. In the onset of Fig. 2 (a), it can be detected when disks are contracting toward each other ($S = -2$), the axial velocity of the Ferro fluid increases alongside an increase in the nanoparticle volume fraction ϕ. Physically we can describe this phenomenon in such a way that when the disks are contracting toward each other, the motion of Ferro fluid molecules becomes faster. Conclusively the axial velocity of the fluid flow increases rapidly. Same behavior can be observed for increasing values of the nanoparticle volume fraction when the disks are at the stationary position ($S = 0$). In case of $S > 0$ (when disks are moving away from each other), it is illustrated that a decline in the axial velocity of the Ferro fluid occurs because of an increase in the nanoparticle volume fraction. In Fig. 2(b), results are devoted for the axial velocity $f(\eta)$ under simultaneous variation of the Hartmann number M and the nanoparticle volume fraction ϕ. It can be determined through Fig. 2(b) within the domain ($0 < \eta < 1$), the graph of the axial velocity oppositely switched its behavior at $\eta = 0.5$ for increasing values of M. Through onset of the plot, it can be analyzed that the axial velocity of the Ferro fluid rises within the domain ($0 < \eta < 0.5$) however behavior of the axial velocity is reversed within the domain ($0.5 < \eta < 1$) for large values of the Hartmann number M. When Fig. 2(a) is closely analyzed, it is found that for $M = 0$, deviation of the axial velocity is almost negligible for various values of the nanoparticle volume fraction ϕ. On the other hand in Fig. 2(b), deviation of the axial velocity shows decreasing behavior within the domain ($0 < \eta < 0.5$) while it is getting a rise in the region ($0.5 < \eta < 1$) for $\phi = 0, 0.1, 0.2$ when the rest of the parameters are fixed. The impacts of squeezing parameter S, Hartmann number M and magnetite particle volume fraction ϕ on the radial velocity $f'(\eta)$ can be disclosed from Fig. 3(a) and (b) respectively. It is examined that the radial velocity $f'(\eta)$ accomplishes decreasing behavior with increasing values of the squeezing parameter S and the Hartmann number M. Furthermore it can be visualized that higher saturation of the magnetite particle volume fraction ϕ gives a rise in the radial velocity $f'(\eta)$ for each value of the squeezing parameter S and the Hartmann number M.

Fluctuation of temperature profile $\theta(\eta)$ for various values of emerging parameters and nanoparticle volume fraction are presented in Fig. 4. Initially in Fig. 4(a) we have drawn a comparison between contraction of disks ($S < 0$) and when the disks are moving apart from each other ($S > 0$). So we have established that when $S = 1$ there is a rapid enhancement in the temperature profile with the increasing values of the nanoparticle volume fraction. However, on the other hand we can observed that for $S = -1$, the results are quite opposite and the temperature profile decreases for increasing values of the nanoparticle volume fraction. Similarly in Fig. 4(b), it can be visualized that influence of the nanoparticle volume fraction along with the Hartmann number gives increasing effects on the temperature profile.

In Figs. 5 and 6, we have plotted the reduced skin friction coefficient and the reduced Nusselt number for various values of emerging parameters. Behavior of the reduced skin friction can be viewed through Fig. 5. It is found in Fig. 5(a) that the reduced skin friction of the fluid near the upper wall is gradually increasing with respect to simultaneous increase of the nanoparticle volume fraction and the squeezing parameter S. We further analyzed that for $\phi = 0.1$, the reduced skin friction near the upper wall is maximum. Similar effects of nanoparticle volume fraction can be observed from Fig. 5(b) in response for reduced skin friction when the values of Hartmann number are gradually increasing. So we can conclude that there is a dominant variation in the reduced skin friction for the squeezing parameter as compared to the Hartmann number. Heat transfer analysis of Ferro fluid near the upper wall is plotted in Fig. 6 through reduced Nusselt number. In Fig. 6(a), we have plotted the reduced Nusselt number against the nanoparticle volume fraction ϕ for non-negative values of the squeezing parameter S. Physically we can say that when the disks are moving away from each other means room will be created between the disks and ultimately the heat transfer among the particles will reduce gradually. Consequence of these effects can be observed through Fig. 6 (a) where increases in the squeezing parameter decrease the heat transfer of the Ferro fluid. Effect of Hartmann number is not

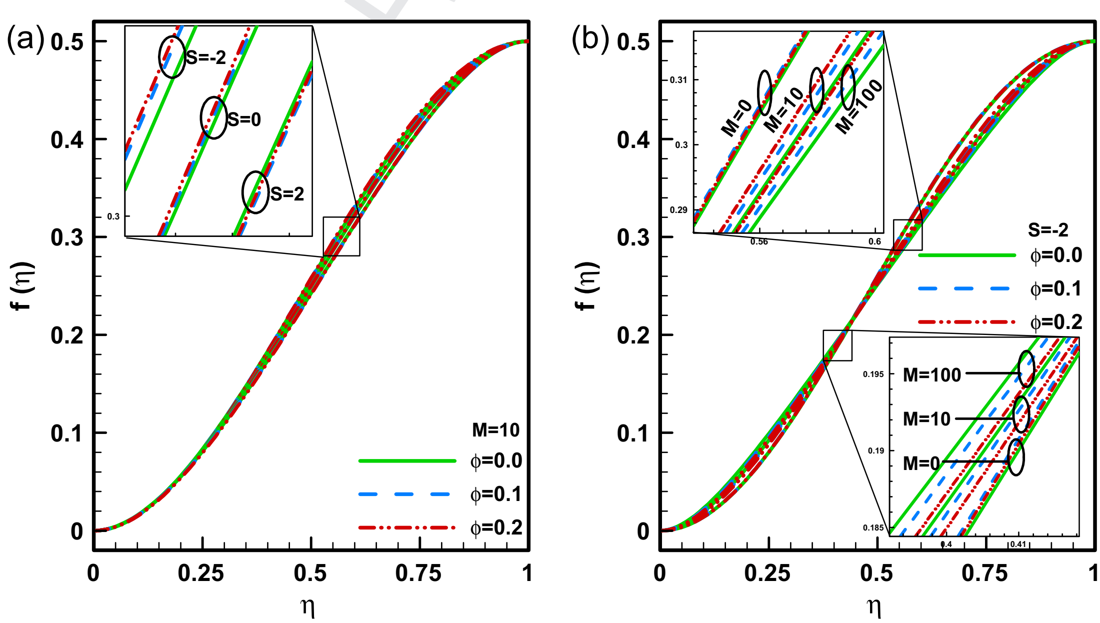

Fig. 2. Variation of axial velocity for (a) squeezing parameter S, (b) MHD parameter M.

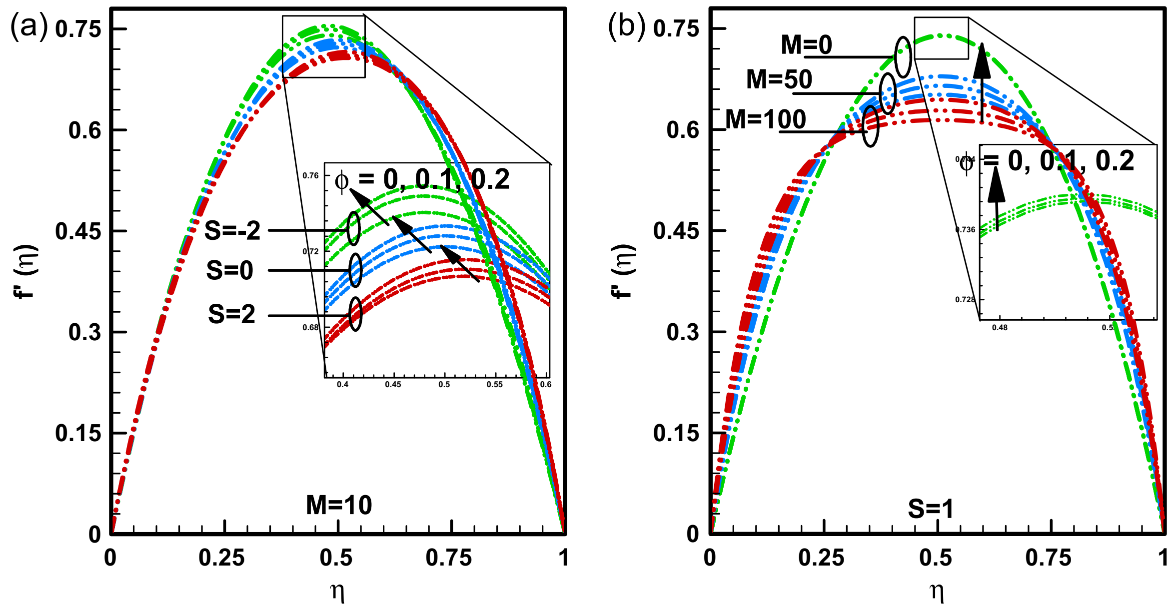

Fig. 3. Variation of radial velocity for (a) squeezing parameter *S*, (b) MHD parameter *M*.

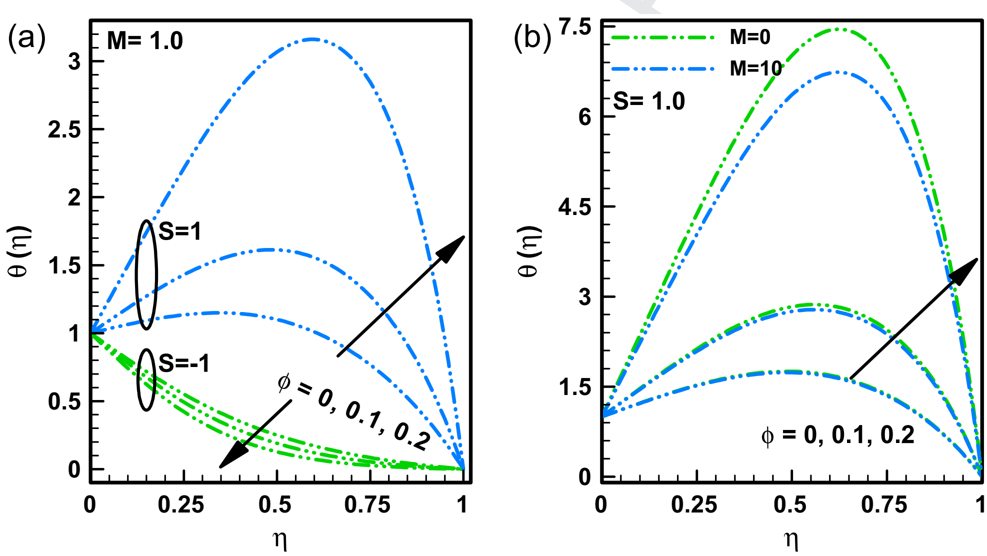

Fig. 4. Variation of temperature profile for (a) squeezing parameter *S*, (b) MHD parameter *M*.

dominating on the local reduced Nusselt number but contradictory behavior can be observed in Fig. 6(b) when it is compared with Fig. 6(a). Moreover, based on Fig. 6, enhancement in the heat transfer is prominent when we increase the nanoparticle volume fraction ϕ.

In order to analyze which nanoparticle gives the highest reduced skin friction and heat transfer at the wall, we simply plotted the comparison among the water based magnetite (Fe_3O_4), cobalt ferrite ($CoFe_2O_4$) and Mn–Zn ferrite (Mn–$ZnFe_2O_4$) particles in Fig. 7. Through Table 1, we can see that the magnetite (Fe_3O_4) particles contain the greatest density as compared to cobalt ferrite ($CoFe_2O_4$) and Mn–Zn ferrite (Mn–$ZnFe_2O_4$). So it can easily be justified that water based magnetite (Fe_3O_4) particles gives the highest reduced skin friction as compared to the rest of the Ferro fluid mixtures (see Fig. 7(a)). Moreover one can see that there is a slight difference between the densities of cobalt ferrite ($CoFe_2O_4$) and Mn–Zn ferrite (Mn–$ZnFe_2O_4$) and so as in Fig. 7(a), the reduced skin frictions of both mixtures remain almost the same for increasing values of the nanoparticle volume fraction. Again in Fig. 7(b), we have plotted the heat transfer among each mixture so we can determine which particle gives the best effect on the reduced Nusselt number. From Table 1, we can see that the magnetite (Fe_3O_4) particles have the best thermal conductivity as compared to the other two particles. So we can see in Fig. 7(b) that the water based magnetite (Fe_3O_4) particles gives the best heat transfer rate as compared to the other mixtures.

In Fig. 8(a) and (b), we have plotted the 3-D isotherms for $S = -1$ and $S = 1$ respectively with different values of the nanoparticle volume fraction. In each figure, we can see that nonzero values of ϕ give higher isotherms as compared to $\phi = 0$. Similarly for $S = 1$, dominant difference and heat transfer in the isotherms are obtained as compared to the case of $S = -1$.

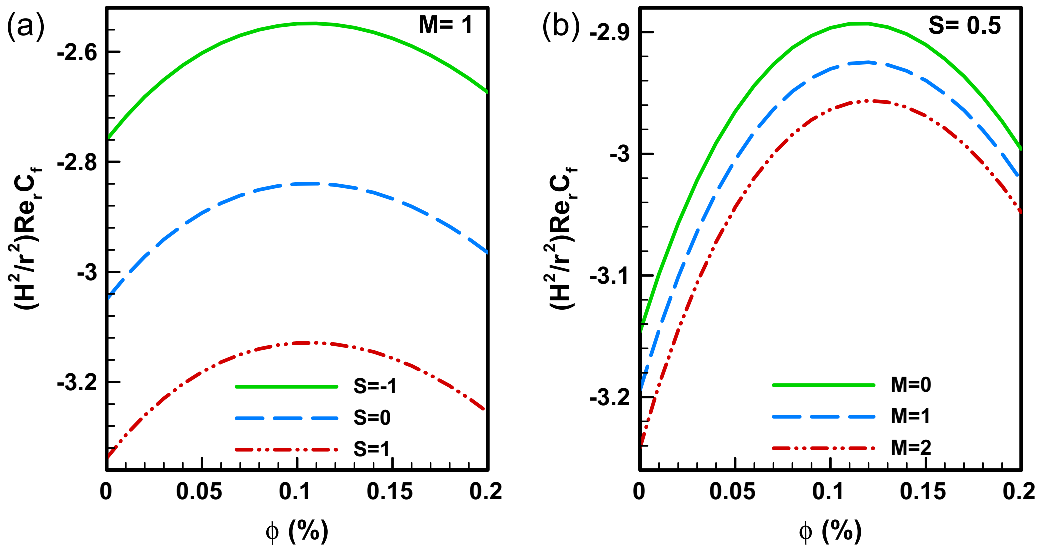

Fig. 5. Variation of reduced skin friction for (a) squeezing parameter S, (b) MHD parameter M.

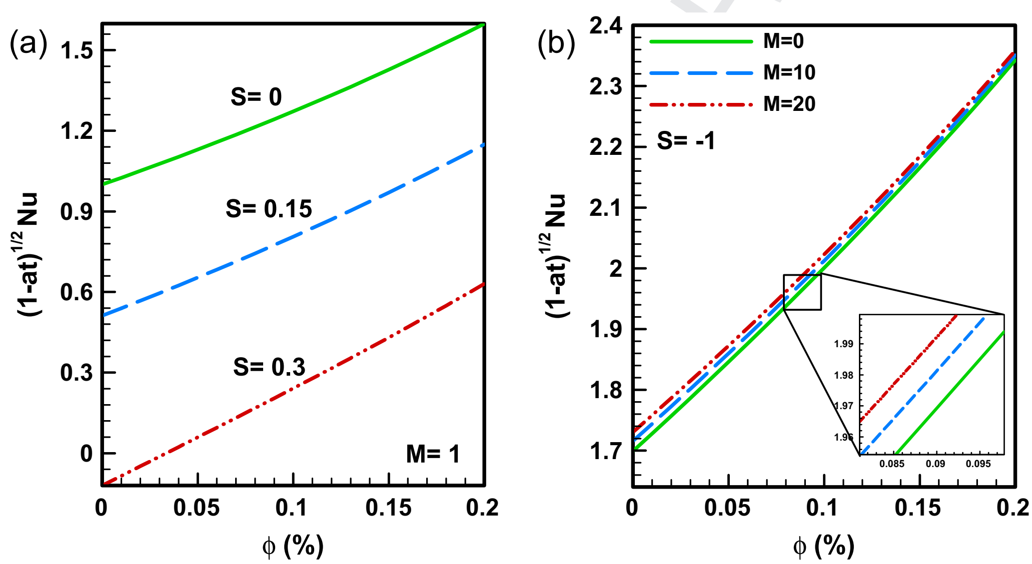

Fig. 6. Variation of reduced Nusselt number for (a) squeezing parameter S, (b) MHD parameter M.

Table 1
Thermophysical properties of base fluids and magnetic nanoparticles as in [43–45].

Physical properties	Water	Fe_3O_4	$CoFe_2O_4$	Mn–$ZnFe_2O_4$
ρ (kg/m^3)	997	5180	4907	4900
C_p (J/kg K)	4179	670	700	800
K (W/m K)	0.613	9.7	3.7	5
Pr	6.2	–	–	–

Table 3
Numerical values of Nusselt number for water functionalized $CoFe_2O_4$ particle with the various values of ϕ, M and S.

$\phi \downarrow$	$S = -1$			$M = 0.5$		
	$M = 0$	$M = 10$	$M = 20$	$S = -0.5$	$S = 0$	$S = 0.5$
0	2.777452	2.796018	2.811913	2.083236	1	−1.34904
0.1	3.171334	3.185215	3.197645	2.398885	1.272139	−0.73676
0.2	3.600019	3.610062	3.619351	2.756950	1.598577	−0.20644

Table 2
Numerical values of skin friction for water functionalized $CoFe_2O_4$ particle with the various values of ϕ, M and S.

$\phi \downarrow$	$S = 0.5$			$M = 1$		
	$M = 0$	$M = 1$	$M = 2$	$S = -1$	$S = 0$	$S = 1$
0	−3.14619	−3.19408	−3.24136	−2.75962	−3.04965	−3.33813
0.1	−2.89646	−2.93013	−2.96348	−2.54915	−2.84010	−3.12930
0.2	−2.99596	−3.02202	−3.04790	−2.67351	−2.96515	−3.25507

Please cite this article in press as: R. Ul Haq et al., Numerical simulation of water based magnetite nanoparticles between two parallel disks, Advanced Powder Technology (2016), http://dx.doi.org/10.1016/j.apt.2016.05.020

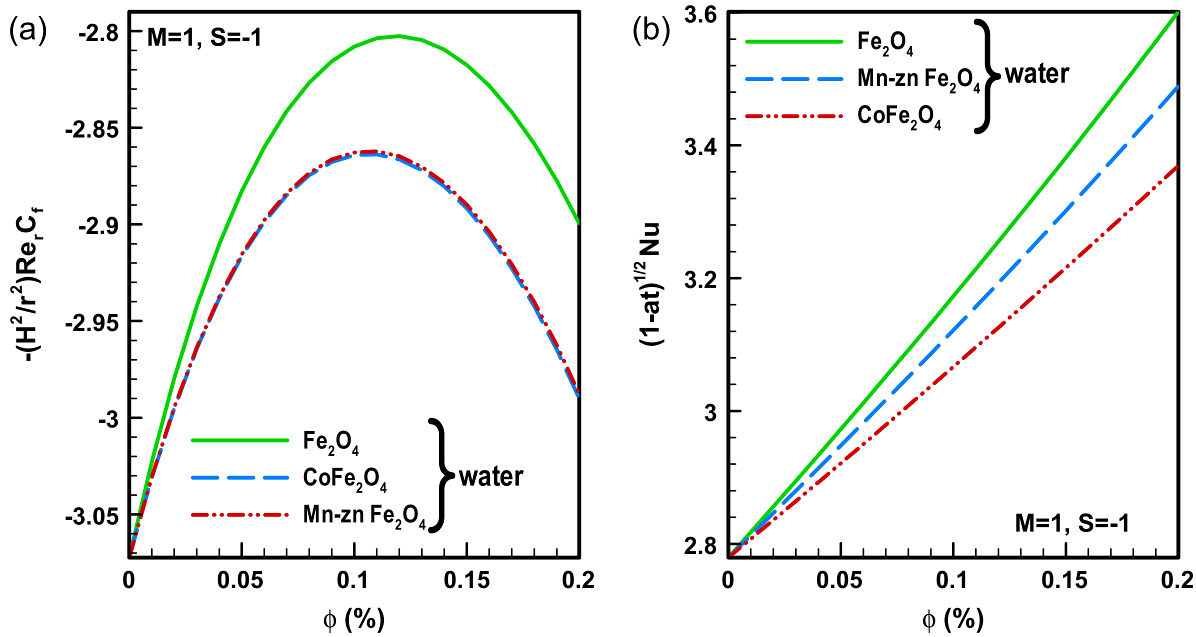

Fig. 7. Comparison among water-based Ferro particles for (a) reduced skin friction, (b) reduced Nusselt number.

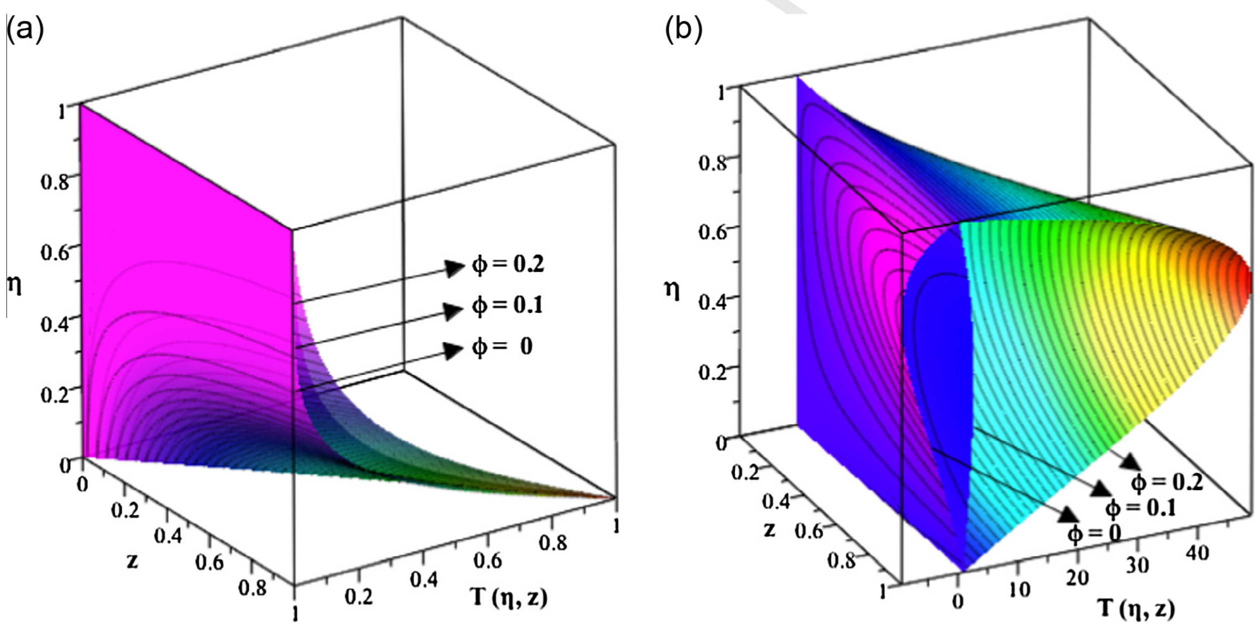

Fig. 8. Isotherms plots for various values of ϕ when (a) $S = -1$, $M = 1$, (b) $S = 1$, $M = 1$.

5. Concluding remarks

Throughout the analysis, simultaneous effect of each Ferro nanoparticles namely magnetite (Fe_3O_4), cobalt ferrite ($CoFe_2O_4$) and Mn–Zn ferrite (Mn–ZnFe_2O_4) within the base fluid have been detected for effective thermal conductivity on temperature and velocity profiles. Dominant effects of squeezing parameter and Hartmann number for each type of nanoparticles have been achieved and discussed in details. Concluding remarks are developed over the result bases and mentioned as follows:

1. For every increasing value of squeezing parameter S and Hartmann number M, velocity profile is gradually decreasing.
2. Increase in the nanoparticle volume fraction ϕ has same increasing effect on velocity profile for each value of S and M.
3. Temperature profile has opposite variation with increasing values of nanoparticle volume fraction for $S > 0$ and $S < 0$.
4. Temperature profile is rising with increasing values of nanoparticle volume fraction ϕ when $M = 0$ and $M = 10$.
5. For the highest value of S and M, the maximum reduced skin friction has been found at the wall for increasing values of ϕ.
6. Water based Ferro magnetite (Fe_3O_4) nanoparticles have low skin friction as compare to the rest of water based nanoparticles. On the other hand Ferro magnetite (Fe_3O_4) provides the higher heat transfer at the surface as compared to the rest of the mixture.

Please cite this article in press as: R. Ul Haq et al., Numerical simulation of water based magnetite nanoparticles between two parallel disks, Advanced Powder Technology (2016), http://dx.doi.org/10.1016/j.apt.2016.05.020

References

[1] S. Ishizawa, The unsteady flow between two parallel discs with arbitrary varying gap width, Bull. Jpn. Soc. Mech. Eng. 9 (1966) 533–550.
[2] R. Usha, R. Sridharan, Arbitrary squeezing of a viscous fluid between elliptic plates, Fluid Dyn. Res. 18 (1996) 35–51.
[3] D. Srinivasacharya, N. Srinivasacharyulu, O. Odelu, Flow and heat transfer of couple stress fluid in a porous channel with expanding and contracting walls, Int. Commun. Heat Mass Transfer 36 (2009) 180–185.
[4] M.M. Rashidi, Hamed Shahmohamadi, Analytical solution of three-dimensional Navier-Stokes equations for the flow near an infinite rotating disk, Commun. Nonlinear Sci. Numer. Simul. 14 (7) (2009) 2999–3006.
[5] M.M. Rashidi, T. Hayat, E. Erfani, S.A. Mohimanian Pour, Awatif A. Hendi, Simultaneous effects of partial slip and thermal-diffusion and diffusion-thermo on steady MHD convective flow due to a rotating disk, Commun. Nonlinear Sci. Numer. Simul. 16 (11) (2011) 4303–4317.
[6] M.M. Rashidi, S.A. Mohimanian Pour, T. Hayat, S. Obaidat, Analytic approximate solutions for steady flow over a rotating disk in porous medium with heat transfer by homotopy analysis method, Comput. Fluids 54 (30) (2012) 1–9.
[7] T. hayat, A. Yousaf, M. Mustafa, S. Asghar, Influence of heat transfer in the squeezing flow between parallel disks, Chem. Eng. Commun. 199 (2012) 1044–1062.
[8] U. Khan, N. Ahmed, S.I. Khan, Z.A. Zaidi, Y. Xiao-Jun, S.T. Mohyud-Din, On unsteady two-dimensional and axisymmetric squeezing flow between parallel plates, Alexandria Eng. J. 53 (2014) 463–468.
[9] U. Khan, N. Ahmed, Z.A. Zaidi, M. Asadullah, S.T. Mohyud-Din, MHD squeezing flow between two infinite plates, Ain Shams Eng. J. 5 (2014) 187–192.
[10] A. Nazir, T. Mahmood, Analysis of flow and heat transfer of viscous fluid between contracting rotating disks, Appl. Math. Model. 35 (2011) 3154–3165.
[11] X.H. Si, L. Zheng, X. Zhang, X. Si, Homotopy analysis method for the asymmetric laminar flow and heat transfer of viscous fluid between contracting rotating disks, Appl. Math. Model. 36 (2012) 1806–1820.
[12] X.H. Si, L. Zheng, P. Lin, X. Zhang, Y. Zhang, Flow and heat transfer of a micropolar fluid in a porous channel with expanding or contracting walls, Int. J. Heat Mass Transfer 67 (2013) 885–895.
[13] S. Srinivas, A.S. Reddy, T.R. Ramamohan, A.K. Shukla, Thermal diffusion and diffusion-thermo effects on MHD flow of viscous fluid between expanding or contracting rotating porous disks with viscous dissipation, J. Egypt. Math. Soc., dx.doi.org/10.1016/j.joems.2014.06.017.
[14] T. Fang, J. Zhang, Y. Zhong, Note on unsteady viscous flow on the outside of an expanding or contracting cylinder, Commun. Nonlinear Sci. Numer. Simul. 17 (2012) 3124–3128.
[15] S.U.S. Choi, Enhancing thermal conductivity of fluids with nanoparticles, in: Developments and Applications of Non-Newtonian flows, FDE 231/MD 66, 1995, pp. 99–105.
[16] J. Buongiorno, Convective transport in nanofluids, J. Heat Transfer 128 (2006) 240–250.
[17] G.C. Bourantas, V.C. Loukopoulos, Modelling the natural convective flow of micropolar nanofluids, Int. J. Heat Mass Transfer 68 (2014) 35–41.
[18] X.Q. Wang, A.S. Mujumdar, Heat transfer characteristics of nanofluids: a review, Int. J. Therm. Sci. 46 (2007) 1–19.
[19] M.M. Rashidi, N.V. Ganesh, A.K.A. Hakeem, B. Ganga, Buoyancy effect on MHD flow of nanofluid over a stretching sheet in the presence of thermal radiation, J. Mol. Liq. 198 (2014) 234–238.
[20] A. Malvandi, D.D. Ganji, Magnetohydrodynamic mixed convective flow of Al_2O_3–water nanofluid inside a vertical microtube, J. Magn. Magn. Mater. 369 (2014) 132–141.
[21] D.A. Nield, A.V. Kuznetsov, The Cheng-Minkowycz problem for natural convective boundary-layer flow in a porous medium saturated by a nanofluid, Int. J. Heat Mass Transfer 52 (2009) 5792–5795.
[22] A.V. Kuznetsov, D.A. Nield, Natural convective boundary-layer flow of a nanofluid past a vertical plate, Int. J. Therm. Sci. 49 (2010) 243–247.
[23] W.A. Khan, I. Pop, Boundary-layer flow of a nanofluid past a stretching sheet, Int. J. Heat Mass Transfer 53 (2010) 2477–2483.
[24] D.A. Nield, A.V. Kuznetsov, The Cheng-Minkowycz problem for the double-diffusive natural convective boundary layer flow in a porous medium saturated by a nanofluid, Int. J. Heat Mass Transfer 54 (2011) 374–378.
[25] T.G. Motsumi, O.D. Makinde, Effects of thermal radiation and viscous dissipation on boundary layer flow of nanofluids over a permeable moving flat plate, Phys. Scripta 86 (2012). 045003(8pp).
[26] O.D. Makinde, Analysis of Sakiadis flow of nanofluids with viscous dissipation and Newtonian heating, Appl. Math. Mech. 33 (12) (2012) 1545–1554 (English Edition).
[27] R. UL Haq, Z.H. Khan, W.A. Khan, Thermophysical effects of carbon nanotubes on MHD flow over a stretching surface, Physica E 63 (2014) 215–222.
[28] R. Ul Haq, S. Nadeem, Z.H. Khan, N.S. Akbar, Thermal radiation and slip effects on MHD stagnation point flow of nanofluid over a stretching sheet, Physica E 65 (2015) 17–23.
[29] R. Ul Haq, S. Nadeem, Z.H. Khan, N.F.M. Noor, Convective heat transfer in MHD slip flow over a stretching surface in the presence of carbon nanotubes, Physica B, http://dx.doi.org/10.1016/j.physb.2014.09.031.
[30] M.M. Rashidi, S. Abelman, N. Freidooni Mehr, Entropy generation in steady MHD flow due to a rotating porous disk in a nanofluid, Int. J. Heat Mass Transfer 62 (2013) 515–525.
[31] O.D. Makinde, W.A. Khan, Z.H. Khan, Buoyancy effects on MHD stagnation point flow and heat transfer of a nanofluid past a convectively heated stretching/shrinking sheet, Int. J. Heat Mass Transfer 62 (July) (2013).
[32] G. Domairry, M. Hatami, Squeezing Cu–water nanofluid flow analysis between parallel plates by DTM-Pade method, J. Mol. Liq. 193 (2014) 37–44.
[33] M. Sheikholeslami, D.D. Ganji, H.R. Ashorynejad, Investigation of squeezing unsteady nanofluid flow using ADM, Powder Technol. 239 (2013) 259–265.
[34] A. Dib, A. Haiahem, B. Bou-said, Approximate Analytical Solution of Squeezing Unsteady Nanofluid Flow, http://dx.doi.org/1016/j.powtec.2014.08.074.
[35] M. Hatami, M. Shiekholeslami, D.D. Ganji, Laminar flow and heat transfer of nanofluid between contracting and rotating disks by least square method, Powder Technol. 253 (2014) 769–779.
[36] M. Hatami, M. Shiekholeslami, D.D. Ganji, Nanofluid flow and heat transfer in an asymmetric porous channel with expanding or contracting wall, J. Mol. Liq. 195 (2014) 230–239.
[37] M. Hatami, D.D. Ganji, Heat transfer and nanofluid flow in suction and blowing process between parallel disks in presence of variable magnetic field, J. Mol. Liq. 190 (2014) 159–168.
[38] Mohsen Sheikholeslami, Kuppalapalle Vajravelu, Mohammad Mehdi Rashidi, Forced convection heat transfer in a semi annulus under the influence of a variable magnetic field, Int. J. Heat Mass Transfer 92 (2016) 339–348.
[39] M. Sheikholeslami Kandelousi, KKL correlation for simulation of nanofluid flow and heat transfer in a permeable channel, Phys. Lett. A 378 (45) (2014) 3331–3339.
[40] M. Sheikholeslami, H.R. Ashorynejad, P. Rana, Lattice Boltzmann simulation of nanofluid heat transfer enhancement and entropy generation, J. Mol. Liq. 214 (2016) 86–95.
[41] M. Sheikholeslami, R. Ellahi, Three dimensional mesoscopic simulation of magnetic field effect on natural convection of nanofluid, Int. J. Heat Mass Transfer 89 (2015) 799–808.
[42] M. Sheikholeslami, Effect of uniform suction on nanofluid flow and heat transfer over a cylinder, J. Braz. Soc. Mech. Sci. Eng. 37 (2015) 1623–1633.
[43] R. Rosensweig, Heating magnetic fluid with alternating magnetic field, J. Magn. Magn. Mater. 252 (2002) 370–374.
[44] H. Oztop, E. Abu-Nada, Numerical study of natural convection in partially heated rectangular enclosures filled with nanofluids, Int. J. Heat Fluid Flow 29–5 (2008) 1326–1336.
[45] B. Weidenfeller, M. Hofer, F. Schilling, Thermal and electrical properties of magnetite filled polymers, Compos. Part A: Appl. Sci. Manuf. 33–8 (2002) 1041–1053.

Please cite this article in press as: R. Ul Haq et al., Numerical simulation of water based magnetite nanoparticles between two parallel disks, Advanced Powder Technology (2016), http://dx.doi.org/10.1016/j.apt.2016.05.020